Nano-scale Shell in Phase Separating Gd-Ti-Al-Co Metallic Glass

Hye Jung Chang*, Eun Soo Park[1], Do Hyang Kim[2]

Advanced Analysis Center, Korea Institute of Science and Technology, Seoul 136-791, Korea
[1]*RIAM, Department of Materials Science and Engineering, Seoul National University, Seoul 151-742, Korea*
[2]*Center for Non-Crystalline Materials, Yonsei University, Seoul 120-749, Korea*

*Correspondence to:
Chang HJ,
Tel: +82-2-958-5365
Fax: +82-2-958-6975
E-mail: almacore@kist.re.kr

In the present study, formation of yard and shell has been investigated in as-melt-spun $Gd_{30}Ti_{25}Al_{25}Co_{20}$ alloy using a variety of transmission electron microscopy techniques. The phase separation during cooling leads to the formation of the microstructure consisting of amorphous droplets with different size scales embedded in the amorphous matrix. Due to the interdiffusion at the interface after the first-step phase separation, ~50 nm-thick yard develops on the surface of the primary droplet particle. Due to the critical wetting phenomenon, ~5 nm thickness shell enveloping the droplet forms. The sell is enriched in Co and Ti, implying that the composition is close to that of the droplet.

Key Words: Metallic glass, Phase separation, Wetting, Shell

INTRODUCTION

Recently, bulk metallic glass receives a great attention since it shows exotic properties such as high strength, high elastic limit and high corrosion resistance (Johnson, 1996). The application of metallic glass considered for structural and functional uses (Hays et al., 2000; Xing et al., 2001; Kim et al., 2003; Lee et al., 2003; Lee et al., 2004; Park et al., 2005; Kim et al., 2011; Lim et al., 2012) has been based on the metallic glass which consists of a single amorphous phase. However, metallic glass which consists of two different amorphous phase can be fabricated when the phase separation in the liquid state is properly retained in the solid state after cooling. In order to design such metallic glasses, two perquisites should be considered: (1) Two different liquid phases should exist in the melt by proper addition of alloying element which has positive enthalpy of mixing with at least one of the constituent elements; and (2) Glass forming ability of the two liquid phases should be enough to ensure the formation of two different amorphous phases in the solid state. So far, the phase separation phenomena have been reported in several glass forming systems (Park et al., 2004; Mattern et al., 2005; Park et al., 2007, Chang et al., 2010). It has been also shown that

droplet or interconnected type microstructure can be formed with two different microstructure formation mechanisms, i.e., spinodal decomposition or nucleation and growth which are determined by the alloy composition (Chang et al., 2010; Park et al., 2004; Park et al., 2006). Design of such phase separating metallic glass may open a new field for structural or functional application of the metallic glass. For example, nano scale powder or foam can be obtained depending on the phase separating microstructure type by proper leaching out of one amorphous phase (Lee et al., 2006a, 2006b; Jayaraj et al., 2009).

As mentioned above, one of the mechanisms of phase separation is nucleation and growth resulting in a droplet type microstructure. When A-B atom pair has positive enthalpy of mixing in the liquid and quenched into miscibility gap region, the system spontaneously separates, thus nucleation and growth of A-rich amorphous droplets occurs in the B-rich liquid melt. Upon cooling, when a particle in the phase separated melt favors one of the components of a mixture, a wetting layer, shell quickly envelops the particle surface by a mechanism of critical wetting suggested by Cahn (1977). This complete wetting can occur at the temperature range between the critical temperature of miscibility gap

and wetting temperature. Such a wetting behavior has been reported intensively in colloidal dynamics, but mostly based on the theoretical calculation. The aim of the present study is to report briefly the microstructure of the shell structure developed during quenching in the as-melt-spun Gd-Ti-Al-Co metallic glass alloy and provide microscopic evidence to understand the wetting mechanism of the phase separating metal alloy in further.

EXPERIMENTAL

Alloy ingots with the nominal compositions $Gd_{30}Ti_{25}Al_{25}Co_{20}$ were made by alloying high-purity elements in an arc furnace under a flowing argon atmosphere. Rapidly solidified ribbons were prepared by re-melting the alloy ingots in quartz tubes, and ejecting then with an over-pressure of 50 kPa through a nozzle onto a copper wheel rotating with a surface velocity of 40 m/s. The resulting ribbons have a thickness of about 40 μm and a width of about 2 mm.

The microstructure of as-melt-spun sample was examined by transmission electron microscopy (TEM) (JEM 2100F; JEOL, Tokyo, Japan) linked with an energy dispersive spectrometer (EDS, Oxford 6498 [Oxford Instruments, Oxfordshire, UK]) and scanning TEM/high annular angle dark field (STEM/HAADF) detector. STEM/HAADF image was acquired with the beam size of 0.2 nm for normal work and 0.7 nm for line scanning. The detection angle for HAADF set to be 80 mrad. TEM foils were prepared from by ion milling (PIPS 691; Gatan, Pleasanton, CA, USA) followed by double-sided Ar^+ ion-beam etching at 2.5 kV acceleration voltage.

RESULTS AND DISCUSSION

Fig. 1A shows the STEM bright field (BF) image and the selected area diffraction pattern (inset) obtained from the as-melt-spun $Gd_{30}Ti_{25}Al_{25}Co_{20}$ alloy. The microstructure consists of droplets with different size scales embedded in the matrix, indicating that phase separation occurred during rapid quenching, forming a droplet type structure due to large positive heat of mixing between Gd and Ti. Two halo rings in the inserted diffraction pattern confirms that two different amorphous phases with different correlation length scales are present. The result of EDS analysis indicated that primary particle with brighter contrast is Ti-rich amorphous phase (average composition; $Gd_5Ti_{47}Al_{15}Co_{33}$), while the matrix with darker contrast is Gd-rich amorphous phases (average composition; $Gd_{51}Ti_9Al_{26}Co_{14}$). The quantitative STEM-EDS results of which the spectrums are not shown here were estimated by averaging the data obtained only from regions where the sample thickness is thin enough to prevent the matrix contribution. To investigate the composition dependence of the contrast of the phases in more detail, HAADF image (Fig. 1B) was acquired from the region marked as a square in Fig. 1A. Since the scattering intensity strongly depends on the atomic number in the HAADF image, Gd-rich matrix appeared with brighter contrast, on the other hand, the primary particle with darker contrast.

By the first-step phase separation, two liquid phases (the droplets and the matrix) of different viscosity form in the liquid melt, and the droplets grow by coalescence of small droplets. However, on further cooling, each liquid phase becomes more supersaturated, hence its compositions continues to diverge until the next-step nucleation of the droplet occurs. Finally, the second-step phase separation takes place, forming small size Gd-rich droplets in the Ti-rich phase and vice versa. The presence of small droplets with brighter contrast in the primary droplet (Fig. 1B) indicates that they are also Gd-rich phase close to the composition of the matrix.
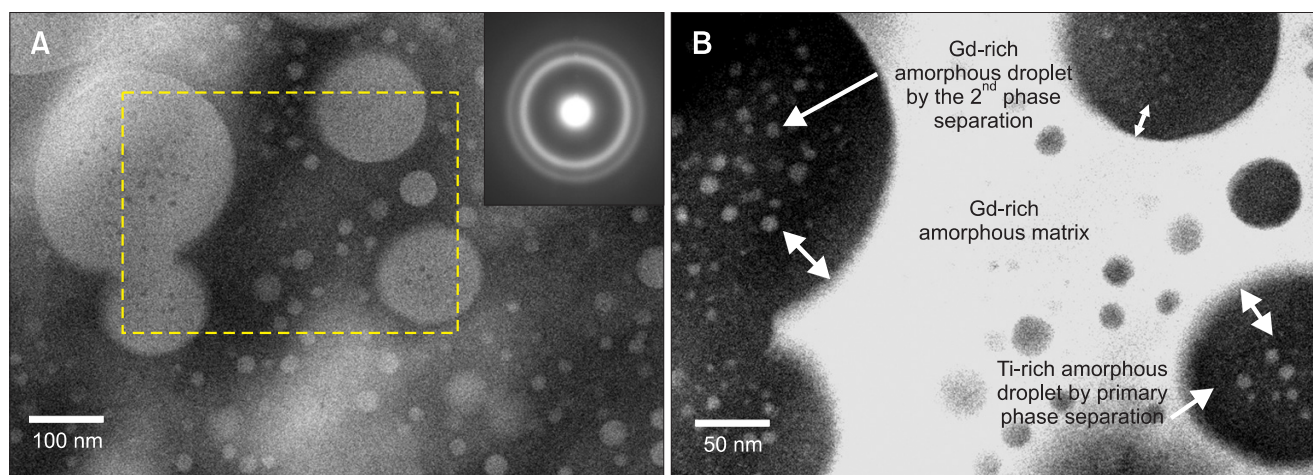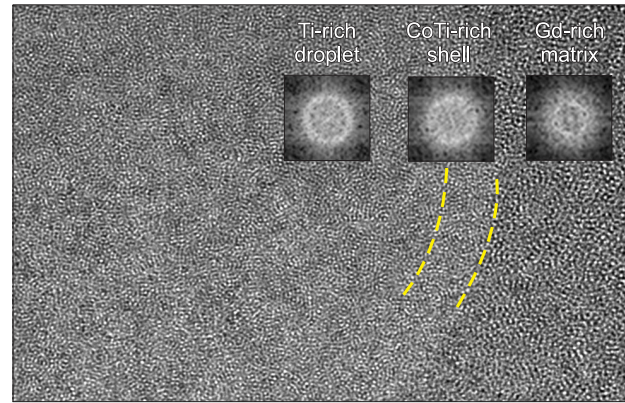

Fig. 1. (A) Scanning transmission electron microscopy bright field image and the selected area diffraction pattern (inset) obtained from the as-melt-spun $Gd_{30}Ti_{25}Al_{25}Co_{20}$ alloy, (B) high annular angle dark field image acquired from the region marked as a square in A.
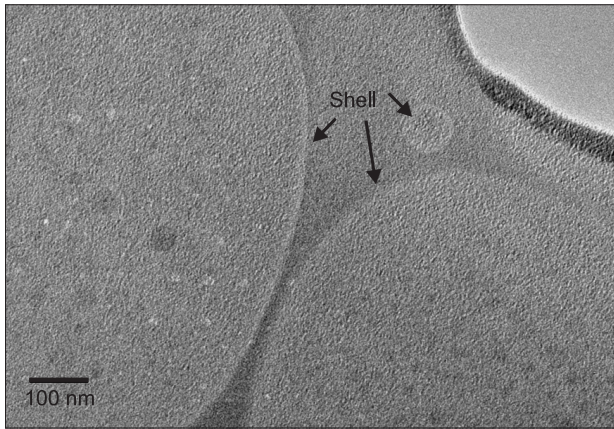
Fig. 2. Transmission electron microscopy bright field image obtained from the as-melt-spun $Gd_{30}Ti_{25}Al_{25}Co_{20}$ alloy.

Fig. 3. High resolution transmission electron microscopy image obtained from the as-melt-spun $Gd_{30}Ti_{25}Al_{25}Co_{20}$ alloy. The Fourier transformed diffraction patterns acquired by from the corresponding area (matrix, shell, and droplet) are inserted in the figure.

Here, it is notable that secondary droplet-free zone develops on the surface of the primary droplet particle with a thickness of ~50 nm (marked with arrows in Fig. 1B). In the same manner, Ti-rich particle did not form in the matrix around the particle. Such an area, referred to as yard appears due to the interdiffusion at the interface after the first-step phase separation. It decreases the supersaturation in each phase, and, as a consequence, small droplets either do not develop in this region or dissolve soon after the development.

In addition to the formation of yard, more detailed examination discloses that ~5 nm thickness shell is enveloping the droplet with brighter contrast compared to that of the droplet inside, which is caused by critical wetting, as shown in the TEM BF image (Fig. 2). The diffraction patterns inserted in the high resolution TEM image (Fig. 3) were acquired by Fourier transformation from the corresponding area (matrix, shell, and droplet). It can be noticed that the average atomic correlation length, that is, the distance which the atomic correlation feature appears and measured by the distance of the diffracted ring from the transmitted origin in selected area diffraction pattern, in Ti-rich droplet is smaller than that in Gd-rich matrix. The average atomic correlation length in the shell was almost close to that of the droplet, but not exactly same. According to EDS results, the composition of the shell ($Gd_{15}Ti_{31}Co_{36}Al_{18}$) was intermediate one between the droplet and the matrix, but rich in Co and Ti as, indicating that the composition of the shell is close to that of the droplet rather than the matrix. Thus, a sharp interface between the shell and the matrix is observed as shown in Fig. 2. However, due to the very fine thickness, it was hard to exactly distinguish the compositional difference in the thin layer. Exact composition analysis of the layer and its formation mechanism will be reported in the forthcoming report.

CONCLUSIONS

The present study shows that the as-melt-spun $Gd_{30}Ti_{25}Al_{25}Co_{20}$ alloy consists of amorphous droplets with different size scales embedded in the amorphous matrix, indicating that phase separation occurred during rapid quenching due to large positive heat of mixing between Gd and Ti. Due to the interdiffusion at the interface after the first-step phase separation, secondary droplet-free zone develops on the surface of the primary droplet particle with a thickness of ~50 nm. Due to the critical wetting phenomenon, ~5 nm thickness shell enveloping the droplet forms. The sell is enriched in Co and Ti, implying that the composition is close to that of the droplet.

ACKNOWLEDGMENTS

REFERENCES

Cahn J W (1977) Critical point wetting. *J. Chem. Phys.* **66**, 3667.

Chang H J, Yook W, Park E S, Kyeong J S, and Kim D H (2010) Synthesis of metallic glass composites using phase separation phenomena. *Acta Mater.* **58**, 2483-2491.

Hays C C, Kim C P, and Johnson W L (2000) Microstructure controlled shear band pattern formation and enhanced plasticity of bulk metallic glasses containing in situ formed ductile phase dendrite dispersions. *Phys. Rev. Lett.* **84**, 2901-2904.

Jayaraj J, Park J M, Gostin P F, Fleury E, Gebert A, and Schultz L (2009) Nano-porous surface states of Ti–Y–Al–Co phase separated metallic glass. *Intermetallics* **17**, 1120-1123.

Johnson W L (1996) Fundamental aspects of bulk metallic glass formation in multicomponent alloys. *Mater. Sci. Forum* **225-227**, 35-50.

Kim S Y, Jee S S, Lim K R, Kim W T, Kim D H, Lee E S, Kim Y H, Lee S M, Lee J H, and Eckert J (2011) Replacement of oxide glass with metallic glass for Ag screen printing metallization on Si emitter. *Appl. Phys. Lett.* **98**, 222112-222112-3.

Kim Y C, Na J H, Park J M, Kim D H, Lee J K, and Kim W T (2003) Role of nanometer-scale quasicrystals in improving the mechanical behavior of Ti-based bulk metallic glasses. *Appl. Phys. Lett.* **83**, 3093-3095.

Lee M H, Bae D H, Kim D H, and Sordelet D J (2003) Synthesis of Ni-based bulk metallic glass matrix composites containing ductile brass phase by warm extrusion of gas atomized powders. *J. Mater. Res.* **18**, 2101-2108.

Lee M H, Lee J Y, Bae D H, Kim W T, Sordelet D J, and Kim D H (2004) A development of Ni-based alloys with enhanced plasticity. *Intermetallics* **12**, 1133-1137.

Lee M H and Sordelet D J (2006a) Nanoporous metallic glass with high surface area. *Scripta Mater.* **55**, 947-950.

Lee M H and Sordelet D J (2006b) Synthesis of bulk metallic glass foam by powder extrusion with a fugitive second phase. *Appl. Phys. Lett.* **89**, 021921-021921-3.

Lim K R, Kim W T, Lee E S, Jee S S, Kim S Y, Kim D H, Gebert A, and Eckert J (2012) Oxidation resistance of the supercooled liquid in Cu50Zr50 and Cu46Zr46Al8 metallic glasses. *J. Mater. Res.* **27**, 1178-1186.

Mattern N, Kuhn U, Gebert A, Gemming T, Zinkevich M, Wendrock H, and Schultz L (2005) Microstructure and thermal behavior of two-phase amorphous No-Nb-Y alloy. *Scripta Mater.* **53**, 271-274.

Park B J, Chang H J, Kim D H, and Kim W T (2004) In situ formation of two amorphous phases by liquid phase separation in Y–Ti–Al–Co alloy. *Appl. Phys. Lett.* **85**, 6353-6355.

Park B J, Chang H J, Kim D H, Kim W T, Chattopadhyay K, Abinandanan T, and Bhattacharyya S (2006) Phase separating bulk metallic glass: A hierarchical composite. *Phys. Rev. Lett.* **96**, 245503.

Park E S, Kim D H, Ohkubo T, and Hono K (2005) Enhancement of glass forming ability and plasticity by addition of Nb in Cu–Ti–Zr–Ni–Si bulk metallic glasses. *J. Non-cryst. Solids* **351**, 1232-1238.

Park E S, Jeong E Y, Lee J K, Bae J C, Kwon A R, Gebert A, Schultz L, Chang H J, and Kim D H (2007) In situ formation of two glassy phases in the Nd-Zr-Al-Co alloy. *Scripta Mater.* **56**, 197-200.

Xing L Q, Li Y, Ramesh K T, Li J, and Hufnagel T C (2001) Enhanced plastic strain in Zr-based bulk amorphous alloys. *Phys. Rev. B* **64**, 180201.